

Ultrasonic-assisted adsorption of Ni(II) ions from aqueous solution onto Fe₃O₄ nanoparticles

Neda Azimi¹, Pedram Azimi², Mohsen Samimi^{*,3}, Tahereh Mansouri Jalilian¹

Received 2nd June 2019,
Accepted 22nd July 2019,
DOI:10.22126/anc.2019.4107.1012

¹ Department of Chemical Engineering, Kermanshah Branch, Islamic Azad University, Kermanshah, Iran

² Bistoon Thermal Power Plant, Kermanshah, Iran

³ Department of Chemical Engineering, Faculty of Energy, Kermanshah University of Technology, Kermanshah, Iran

Abstract

This paper focused on the study of the impact of ultrasonic waves on the intensification of Ni(II) removal from aqueous solution by adsorption onto Fe₃O₄ nanoparticles. Co-precipitation method was used to synthesis Fe₃O₄ magnetic nanoparticles (MNPs) and the average size of the nanoparticles was obtained about 19 nm by SEM. Two layouts including shaker and ultrasonic irradiation are examined. The effects of pH, adsorbent mass and initial concentration of Ni(II) on the removal efficiency of Ni(II) were investigated. The Ni(II) removal efficiency had the highest value at pH=9. Ni(II) removal from aqueous solution using ultrasonic need to lower contact time than the shaker at identical conditions. The highest removal efficiencies of Ni(II) were 83.3% and 85.5% with the contact times of 100 minutes and 60 minutes, respectively using the shaker and ultrasonic. Finally, Langmuir and Freundlich isotherms were employed to correlate sets of experimental adsorption isotherm data. The fitting results showed that non-linear Langmuir model could fit the data better than Freundlich model.

Keywords: Nickel, Fe₃O₄, Nanoparticles, Ultrasonic, Adsorption.

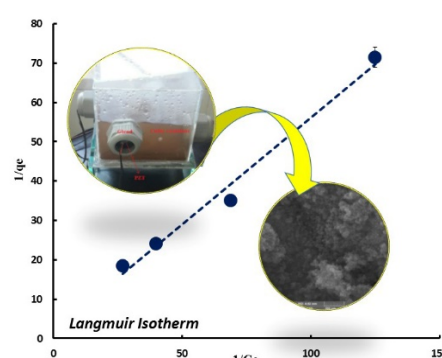
Introduction

Heavy metals are among the most important pollutants that enter into the environment through industrial activities. Nickel (Ni) as one of the toxic metals is characterized as the group of human with carcinogens agents by the United States Environmental Protection Agency.¹⁻⁵ Ni(II) species are highly soluble, mobile, and toxic. Increasing demand for Ni(II) in various industrial applications such as battery production, electroplating, smelting, mineral processing, etc., leads to more discharge of Ni(II) in wastewater, which is harmful to human health and the environment.⁶⁻⁹ For this purpose, strict and precise instructions have been situated for discharge of Ni(II) into surface waters. Adsorption is one of the important techniques of separation processes in many natural, physical, biological, and chemical industries, because of the high capability of solid substances to attract the molecules of gases or solutions. In recent years, the adsorption process has been used as one of the best methods for the removal of metal ions, which is preferred to other methods because of its easy to use and low cost.¹⁰ However, the adsorption process has a low mass transfer rate, difficulty to the regeneration with the adsorbent and limitations for development and application.¹¹ To overcome this weakness, some modifications to the conventional adsorption process have been extensively investigated. Ultrasonic is a new green technology that can intensify chemical and the mass transfer

processes and break the bonded between the adsorbate and the adsorbent.¹¹⁻¹³ These effects are because of the phenomena of shock waves, acoustic cavitation, and microstreaming. The shock waves induce the microscopic turbulence within interfacial films surrounding solid particles. Acoustic cavitation is the formation, growth, and the collapse of micrometer-scale bubbles generated by the propagation of ultrasonic wave into a liquid medium. Acoustic microstreaming produced by the ultrasonic waves is the foundation movement of the liquid.¹⁴⁻¹⁶ These phenomena originated from the ultrasonic energy in adsorption processes, results in the increase in the rate of mass transfer near the surface of the adsorbent. In addition, when nanoparticles used as adsorbents for the adsorption of metal ions, propagation of ultrasonic into aqueous solution can break up the aggregates of nanoparticles into a stable and homogeneous suspension because it has high energy density. Furthermore, ultrasonic acts like an agitator or a mixer and can apply the strong mechanical forces in the solution, so; it can intensify the mass transfer rate in the solid-liquid interface.^{17,18}

Schueller and Yang¹⁹ investigated the impact of ultrasonic on the adsorption and desorption of phenol using activated carbon and polymeric resin. They reported that for the adsorption process in a batch adsorber, ultrasonic act as a mixer and improve the mass-transfer coefficient owing to the generation of cavitation and acoustic streaming.

Wu et al.²⁰ assessed the effect of ultrasonic on the adsorption and desorption processes of blueberry anthocyanins on macropor-



Corresponding author:
Mohsen Samimi, Email: m.samimi@kut.ac.ir

ous resins. Their results show that ultrasonic mainly improved the adsorption process by increasing the surface roughness of the resin surfaces and strengthening the formation of hydrogen bonds. In another work, Mehrabi et al.²¹ used a novel adsorbent for the ultrasonic energy-assisted adsorption of Ni(II) ions from aqueous solution. In this work, Langmuir, Freundlich, Temkin, and Dubinin-Radushkevich isotherm models analyzed the experimental data and the equilibrium data fitted very well in Langmuir isotherm equation.

In all of the above-mentioned researches, it is illustrated that the mass transfer rate and adsorption process are enhanced by the presence of ultrasonic. It should be noted that in most of these works, low-frequency ultrasonic waves are used in order to improve the adsorption process. The application of the ultrasonic waves in the frequency spectrum above 1 MHz in mass transfer processes is limited in the literature. The ultrasonic waves in the range of MHz are able to generate more intense acoustic streaming which is responsible for mass transfer rate augmentation. The main difference of this work with the mentioned references^{1,7,8,19,21} is that the experiments undertaken in the present study are the adsorption of Ni(II) ions onto a sorbent while this process is intensified by sonication under the high-frequency ultrasound waves (1.7 MHz). Regarding the author's literature survey, there are not any studies concerning the influences of the high-frequency ultrasound waves on the adsorption process in a sono-container. In this contribution, the purpose of this study is the investigation of using ultrasonic technology for Ni(II) removal from aqueous solution and adsorption onto Fe₃O₄ nanoparticles. The effects of five independent variables such as the initial concentration of Ni(II) ions, initial pH of the solution, adsorbent mass, and ultrasonic time on the adsorption, as well as equilibrium adsorption isotherms and kinetics models are analyzed.

Experimental

Experimental setup and apparatus

A real photograph of the cubic container equipped with five ultrasonic transducers (namely sono-container) used in the present work is depicted in Figure 1. The main body of the sono-container, which is a cubic container, is fabricated from Plexiglass plates (10 cm×10 cm). The volume of the sono-container is about 1 liter. A Plexiglass cube with the dimension of 15 cm×10 cm×7 cm as the base is located in the bottom of the sono-container. Five piezoelectric transducers (PZT) with a diameter of 2.5 cm and a frequency of 1.7 MHz are located on the body of the sono-container. So, four PZTs are located on the body of each vertical face and one of them is placed on the center of the bottom plate of the sono-container. This arrangement lead to the PZTs do not face each other; the streams created by the PZTs have not collided together. Five PVC keepers known as Glend are used to place the PZTs on the body of the sono-container.

Scanning electron microscopy (SEM, Philips model XL30) is used to produces images of a sample by scanning the surface with a focused beam of electrons. A flame atomic absorption spectroscopy (Thermo model) with a nickel hollow-cathode-lamp, an operating current of 8 mA and wavelength and spectral bandwidth of 232.0 and 0.2 nm, respectively, is used to determine the recovery rate of Ni(II) adsorption.

Preparation of solution

In all experiments, deionized water (DI-water) was used to make the processes more efficient. A stock solution of Ni(II) is prepared by dissolving Ni(NO₃)₂·6H₂O in DI-water, and that solution is

diluted to the desired concentration for actual use. Firstly, 100 mg of Ni(NO₃)₂·6H₂O powder is dissolved in 1 liter of DI-water in a separate container (initial concentration of 100 mg/L). Then, by using a shaker at 150 rpm, the desired solution at room temperature (25°C) is completely mixed. In order to determine the effect of pH, NaOH and HCl solutions with 0.1 molar concentrations are used and pH is measured using pH meter (model: Eutech pH 700, Singapore). In this study, the effect of adsorbent dose (Fe₃O₄ magnetic nanoparticles) on the removal of Ni(II) ions from the base solution is investigated. The adsorbent dose is investigated as a variable with the domain of 2-10 g (2, 4, 6, 8 and 10) Fe₃O₄ nanoparticles. In order to make any solution, a certain amount of adsorbent dissolved in a solution containing Ni(II) ions. At this step, each solution containing Ni(II) ions and adsorbent at five different pH values of 2, 4, 7 and 9 are investigated.

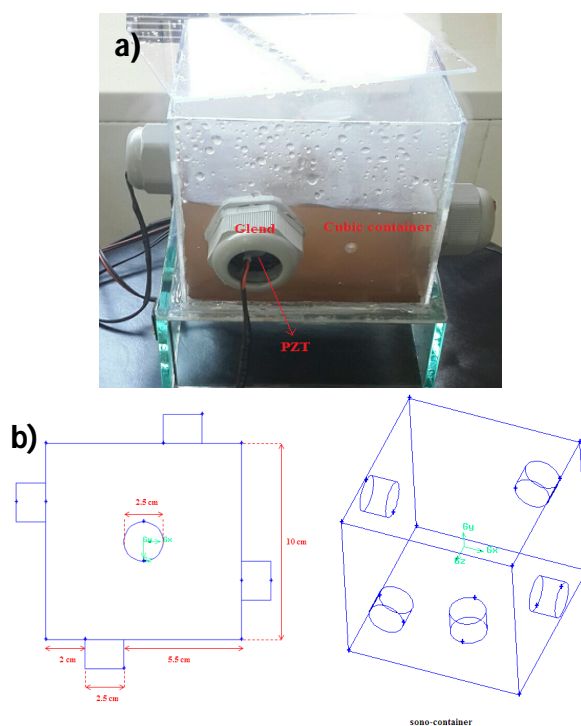
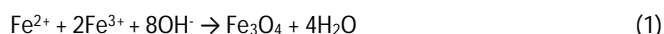


Figure 1. (a) Real photograph and (b) schematic diagram of the experimental setup used in the present work.

Preparation of Fe₃O₄

The synthesis approaches of Fe₃O₄ nanoparticles are reported elsewhere,^{22,23} and the basis of these methods is relying on the co-precipitation method. In summary, the synthesis of Fe₃O₄ nanoparticles by co-precipitation method is given below (equation (1)):



FeCl₃·6H₂O and FeCl₂·4H₂O salts are supplied by Merck Inc to precipitation of Fe³⁺ and Fe²⁺ and ammonium hydroxide (NH₄OH, 28%) is provided by Fluka.

2.7 g of FeCl₃·6H₂O and 1 g of FeCl₂·4H₂O salt were dissolved in 120 mL deionized water. Then, 11 mL of ammonium hydroxide (28%) was added to the mixture of FeCl₃·6H₂O, FeCl₂·4H₂O and DI water under intensive stirring. The temperature of the reacting sample in a water bath is kept at 60°C for one hour while it was under intensive stirring. In addition, it was dispersed by sonicator

for 30 min. As Fe₃O₄ nanoparticles were formed, the solution became black. So, the synthesized Fe₃O₄ nanoparticles were transmitted to a beaker and separated from liquor with a strong magnet. Nanoparticles were washed several times with deionized water until the pH value reached 7.0. Finally, nanoparticles were collected in a vacuum drying chamber after drying at 60°C for 4 hours.^{22,23} The average size of the nanoparticles is obtained about 19 nm by scanning electron microscopy as shown in Figure 2.

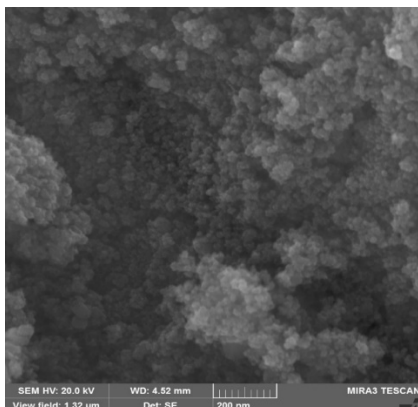


Figure 2. SEM image of the synthesized Fe₃O₄ nanoparticles.

Experiment procedure

In this study, the experiments are carried out in two layouts. Firstly, a solution containing Ni(II) ions and the sorbent is poured into a 1-liter beaker similar to a sono-container and placed on a shaker at 400 rpm for a specified period. The solution is then passed through a Whatmen filter with the size of 0.45 microns (made in Germany) to remove all magnetic nanoparticles. Then, the solution is analyzed by atomic absorption spectroscopy to determine the recovery rate of Ni(II) adsorption.

Secondly, in order to investigate the effect of high-frequency ultrasonic waves on Ni(II) adsorption, the previous experiments in the layout of using shaker are repeated in the sono-container. One liter of suspension containing Ni(II) ions and adsorbent are poured into the sono-container, the piezoelectric actuator switched on ultrasonic transducers, and the ultrasonic waves propagate into the solution. The solution is subjected to ultrasonic waves for a specified period. In the presence of high-frequency ultrasonic waves, the need for mixing with a mechanical stirrer will be eliminated. After the prescribed time, the solution is removed from the sono-container and finally, the solution is passed through a Whatmen filter to remove the nanoparticles. It should be noted that instead of Whatmen filter, it could use of permanent magnets for separation of magnetic nanoparticles.

So that, all Fe₃O₄ nanoparticles are taken with the Whatmen filter and the solution is free of adsorbent. Then, the solution is analyzed to determine the mass transfer rate of Ni(II) in adsorption process. All experiments are carried out at room temperature and each experiment is repeated three times, and the average of the three obtained values is reported as the final amount of adsorbed Ni(II) ions.

Experimental data processing

When the time of the adsorption is long enough, the adsorption system reaches to an equilibrium state and thus the equilibrium amount adsorbed of Ni(II) ions can be calculated by equation (2)^{21,24}:

$$q_e = \frac{C_0 - C_e}{m} V \quad (2)$$

where q_e is the absorption capacity of Ni(II) ions in the equilibrium state, C_0 and C_e are the initial and equilibrium concentration of Ni(II) ions in solution, respectively. V is the volume of solution, and m is the adsorbent mass.

The removal efficiency of Ni(II) ions is calculated by equation (3)^{21,24}:

$$\text{Removal efficiency} = \frac{C_0 - C_t}{m} \times 100 \quad (3)$$

where C_0 and C_t are the ion concentration at initial and after time t , respectively.

Results and discussion

Effect of pH on the adsorption of Ni(II) ions

pH is a key factor in the adsorbing of heavy metal ions from solutions. Therefore, pH dependence is investigated for the removal of Ni(II) ions at a constant contact time in both layouts of using the shaker and ultrasonic waves. Figure 3 shows the percentage removal of Ni(II) ions from the solution using the shaker and the sono-container at the temperature of 25°C, adsorbent mass (m) of 2 g, and the different contact times. At this step, all PZTs on the body of the sono-container switched on and the ultrasonic waves propagated into the sono-container. As shown in Figure 3, for both layouts, the efficiency of Ni(II) removal increased from 2 to 9 and it has the highest amounts of Ni(II) removal at pH=9. In fact, pH is one of the most important parameters for the controlling of the metal-ion adsorption processes.

There are two main factors influencing the effect of pH on the adsorption of metal contaminants on the magnetic nanoparticles. One of them is the metallic pollutant ion, and the other is the surface of adsorbent. In this section, the effect of pH on each of these factors investigated separately. The surface of Fe₃O₄ nanoparticles has a negative charge. In order to have a high adsorption capacity, the pollutant must have a positive charge. Fe₃O₄ nanoparticles can easily be converted to iron hydroxide (II) and (III). In order to investigate the effect of pH on the metal contaminants, it should be noted that the metal in the acidic environments are ionic and when they enter in the base environment, they lose their ionic state and react with the OH⁻ groups in the environment. This process causes the metal to lose its positive charge and become neutral or negative (in the complexation between metal and OH⁻ groups). Therefore, according to the mentioned factors, there is only a small range of acid-to-base pH, in which the amount of metal ion adsorption on the surface of adsorbent is high. Optimization studies showed that the optimal pH value is about 9, which indicates that at this pH, the magnetic adsorbent and nickel metal ions are completely active in the environment.^{25,26} According to Figure 3, it can be seen that with increasing pH, the amount of Ni(II) ion adsorption has increased, so that at pH=9 and pH=2, the maximum and the minimum values have been obtained, respectively. The comparison between Figure 3 (a) and (b) shows that with increasing contact time from 40 min to 80 min, the removal percentage of Ni (II) ions in the shaker increased while for the use of the sono-container it decreased. Therefore, the contact time is an important parameter and should be investigated further. In the next section, the effect of this parameter is evaluated.

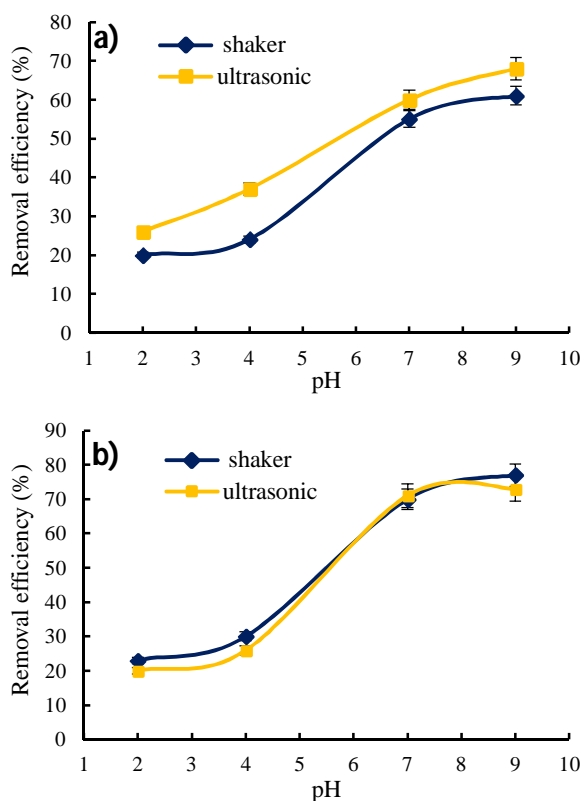


Figure 3. Removal efficiency of Ni(II) using shaker and ultrasonic at $T = 25\text{ }^{\circ}\text{C}$ and $m = 2\text{ g}$ at (a) $t = 40\text{ min}$, (b) $t = 80\text{ min}$.

Effect of contact time on the adsorption of Ni(II) ions

Figure 4 shows the time-dependent removal behavior of Ni(II) ions from aqueous solution using magnetic adsorbent. As shown, for both layouts, the amount of Ni(II) removal increases with increasing the contact time and the equilibrium time from 10 min to 100 min. However, with regard to the use of the shaker, the removal percentage of Ni(II) ions from the contact time between 10 min and 60 min are still increasing and in 80-90 min, the removal percentage approximately is equal. In fact, the removal percentage of Ni(II) ions in the shaker have reached its maximum value of 78% within 100 min.

Initially, the adsorption process of Ni(II) ions is very fast due to a large number of sites on the nanoparticles. According to the results obtained for using the shaker, the contact time of 100 min is chosen as the most effective contact time to remove Ni(II) ions. However, as shown in Figure 4, in the case of the sono-container, the removal percentage of Ni(II) is very fast in the first 10-100 minutes, and its maximum value at contact time of 60 min reached to 76% and after that, the removal percentage of Ni(II) ions have been constant. In fact, the adsorbent surface and its sites initially increased by ultrasonic propagation in the solution. This means that high-frequency ultrasonic waves can produce high percentages of removal of Ni(II) from aqueous solution, due to the creation of micro-streams and acoustic cavitation phenomena. The application of ultrasonic waves into the sono-container increases the adsorption rate over a short time using a small amount of adsorbent material.

Ultrasonic through secondary activities such as cavitation (nucleation, growth, and temporary collapse of small gas bubbles) increases the mass transfer through the physical phenomena such as micro-streams, micro-turbulences, acoustic waves (or shock), and micro-jets.^{15,16} These phenomena occurred without significantly altering the equilibrium properties of the adsorption

/desorption system.²¹ According to the results obtained for using the sono-container, the contact time of 60 min selected as the most effective contact time for the removal of Ni(II) ions under the influence of high-frequency ultrasonic waves.

There are many parameters that can affect the adsorption rate of Ni(II) ions, such as structural properties of the sorbent (Fe_3O_4 nanoparticles), Ni(II) ion properties, initial concentration of Ni(II) ions, temperature, and complex formation rate. It is known that sorption kinetics is dependent or controlled by different kinds of mechanisms such as mass transfer, diffusion control, chemical reactions, and particle diffusion. In order to explain the kinetic characteristics of the sorption, three well-known kinetic models are used to consider the experimental data. For this purpose, the Lagergren's pseudo-first-order kinetic model, the pseudo-second-order kinetic model, and the intraparticle diffusion model are used.²⁷

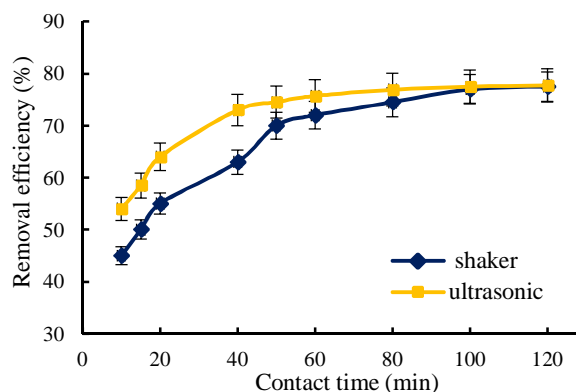


Figure 4. Influence of contact time on the removal efficiency of Ni(II) using shaker and ultrasonic at $T = 25\text{ }^{\circ}\text{C}$, $m = 2\text{ g}$, and $\text{pH} = 9$.

First-order kinetics

The linearized form of the first-order rate equation presented by Lagergren and Svenska is as follow²⁷:

$$\log(q_e - q_t) = \log(q_e) - \frac{k_{\text{ads}}t}{2.303} \quad (4)$$

where q_e and q_t are the amounts of Ni(II) ion adsorbed (mg/g) at equilibrium and at time t (min), respectively and k_{ads} is the sorption rate constant (min^{-1}). The plot of $\log(q_e - q_t)$ versus t gives a straight line and the rate constants (k_{ads}) and theoretical equilibrium sorption capacities, q_e (theory), can be calculated from the slopes and intercepts.

As depicted in Figure 5, the straight lines obtained from Lagergren plots suggest the applicability of the pseudo-first-order kinetic model to fit the experimental data. However, it is also required that theoretically calculated equilibrium sorption capacities, q_e (theory), should be in accordance with the experimental sorption capacity, q_e (exp.) values. Constants related to this plot are given in Figure 5. Linear correlation coefficients of the plot for shaker and ultrasonic are good. The values for shaker, q_e (theory=0.0766) and q_e (exp.=0.076) approximately are in agreement with each other. In addition, the values for ultrasonic, q_e (theory=0.0777) and q_e (exp.=0.0767) are in acceptable agreement with each other.

Second-order kinetics

The experimental data are also applied to the pseudo-second-order kinetic model, which is given with the following equation²⁷:

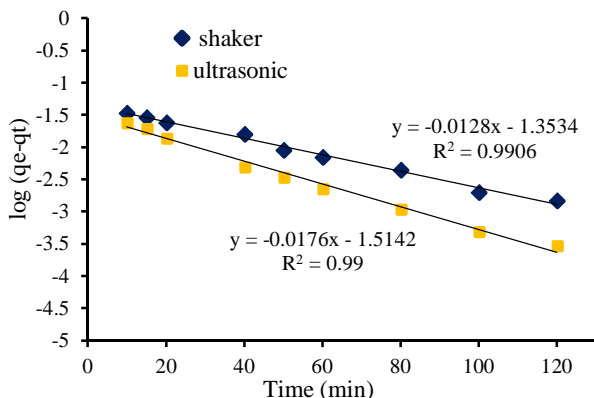


Figure 5. The pseudo-first-order reaction plot for Ni(II) adsorption capacity onto Fe₃O₄ nanoparticles (*T* = 25 °C, *pH* = 9, *m* = 2 g).

$$\frac{t}{q_t} = \frac{1}{(k_2 \cdot q_e^2)} + \frac{t}{q_e} \quad (5)$$

where *k* (g mg⁻¹ min⁻¹) is the rate constant of pseudo-second-order sorption reaction. Second-order kinetic is being applicable if the plot of *t/q_t* versus *t* shows linearity. Figure 6 depicted the plots obtained from the graphical interpretation of the data for the second-order kinetic model. As can be seen from the results given in Figure 6, correlation coefficients are higher compared to the results obtained from the first-order kinetics. Also, theoretical and experimental *q_e* values are in very good accordance with each other. So, it is possible to suggest that the sorption of Ni(II) metal ions onto Fe₃O₄ followed second-order type reaction kinetics.

Intraparticle diffusion

The intraparticle diffusion model is expressed with the equation given by Weber and Morris²⁷:

$$q_t = k_{id} \cdot t^{\frac{1}{2}} \quad (6)$$

where *q_t* is the amount of Ni(II) ions adsorbed at time *t* (mg/g), *k_{id}* is the intraparticle diffusion rate constant (mg/g (min^{1/2})⁻¹).

The Webber and Morris plot for Ni(II) adsorption process is given in Figure 7. It is obvious that the plot in Figure 7 is divided into three regions. The initial region describes a rapid adsorption stage that is external surface adsorption. The second stage is the moderate adsorption stage that belongs to the intraparticle diffusion process and the third zone belongs to the final equilibrium stage. In this step, the intraparticle diffusion extremely declines due to decrease of solute concentration. Therefore, the adsorption process achieves the equilibrium condition gradually. The high regression coefficient values showed a poor fitting between Ni(II) adsorption data with Weber Morris model.

Effect of adsorbent mass on the adsorption of Ni(II) ions

In order to investigate the effect of adsorbent mass on the Ni(II) ions adsorption process, four values for adsorbent containing 2, 4, 6, 8 and 10 g of magnetic nanoparticles in two liters of Ni(II) solution are tested. Figure 8 shows the effect of adsorbent mass on the Ni(II) ion removal from aqueous solution for both layouts of the using the shaker and the sono-container (PZTs with the frequency of 1.7 MHz). Based on this Figure, the adsorption rate of Ni(II) in the high amount of adsorbent increased due to increasing its surface area. Increasing the specific area and the availability of more active adsorbent sites in a higher amount of adsorbent is associated with

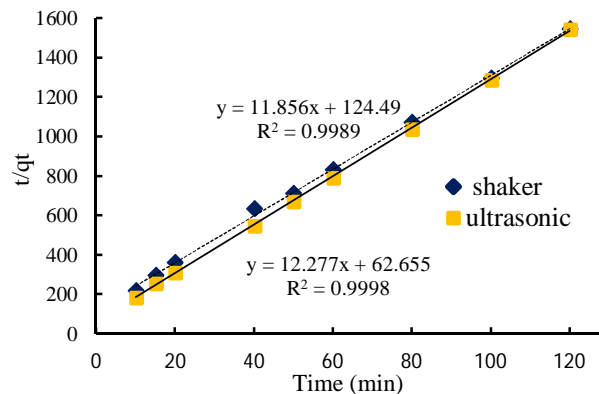


Figure 6. The pseudo-second-order reaction plot for Ni(II) adsorption capacity onto Fe₃O₄ nanoparticles (*T* = 25 °C, *pH* = 9, *m* = 2 g).

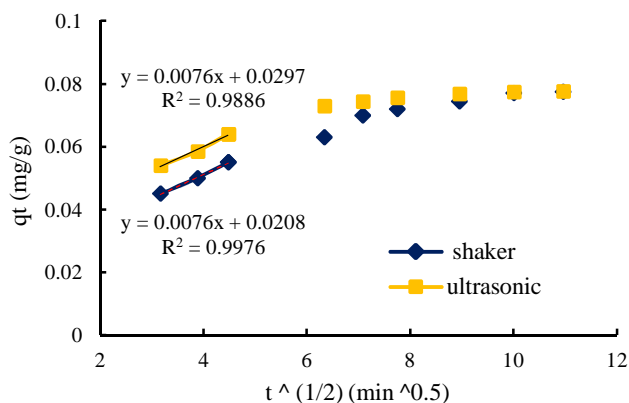


Figure 7. Intraparticle diffusion plot for Ni(II) adsorption capacity onto Fe₃O₄ nanoparticles (*T* = 25 °C, *pH* = 9, *m* = 2 g).

an increase in adsorption rate. By using the shaker and the sono-container, the highest removal percentages of Ni(II) are 83.3% and 85.5%, respectively, with the contact times of 100 min and 60 min, respectively. These contact times were selected as the efficient contact times due to achieving the highest removal percentages of Ni(II) ions.

In both cases, the efficient adsorbent dose is *m* = 6 g and no significant increase in removal efficiency is observed with increasing adsorbent dose of more than 6 g. Considering that in all of the above experiments, the sono-container with a shorter contact time compared to the shaker, performed better in removing Ni(II) ions from aqueous solution, so in the next experiments, the sono-container is used.

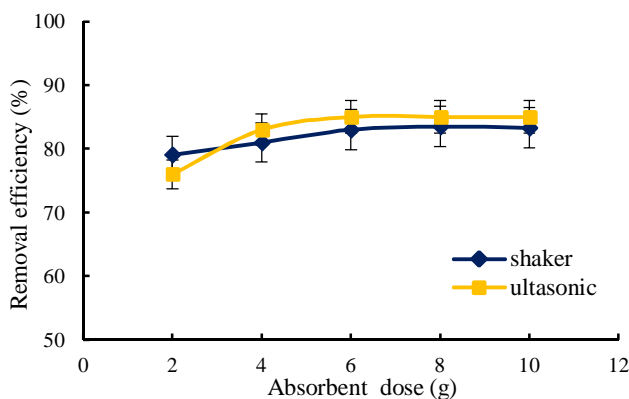


Figure 8. Influence of adsorbent mass on the removal efficiency of Ni(II) using shaker and ultrasonic at *T* = 25 °C and *pH* = 9.

Effect of initial concentration of Ni(II) ions on the adsorption process

The effect of initial nickel concentration is another parameter that studied for the removal of Ni(II) by magnetic nanoparticles.²¹ In all experiments in the before sections, the initial concentration of Ni(II) is 0.1 g/L. In this section, three concentrations including 0.05 g/L, 0.15 g/L and 0.2 g/L are investigated. Figure 9 shows the effect of the initial concentration of Ni(II) ions in the aqueous solution on its percentage removal at $m=6$ g and $pH=9$ while all PZTs are activated. In this Figure $m=6$ is selected as adsorbent dose, because according to Figure 8, the efficient dose of adsorbent is 6 g and no significant increase is observed with increasing adsorbent dose of more than 6 g for Ni(II) removal.

From Figure 9, it can be concluded that there is a high dependency between the removal efficiency and the initial concentration of Ni(II) ions. So, by increasing the initial concentration, the available adsorbent sites are reduced and, as a result, the removal efficiency decreases.¹⁴ Since in the low concentration, available sites to the adsorbent surface are greater.¹⁴ As shown in Figure 9, by an increase in the concentration of Ni(II) ions from 0.05 to 0.1 g/L, the percentage of Ni(II) ions decreased from 84% to 85.5%, respectively. While by increasing Ni(II) from 0.1 to 0.15 and 0.2 g/L, the percentage of Ni(II) ions has decreasing trend, which is due to the reduction of the adsorption capacity of Ni(II) by nanoparticles and filling their capacity. By increasing the initial concentration of Ni(II) ions in the solution, the removal efficiency is reduced. Increasing the initial concentration of Ni(II) ions causes less adsorbed sites to adsorb more nickel in the solution. Therefore, the adsorbent in lower initial concentration has better adsorption properties.

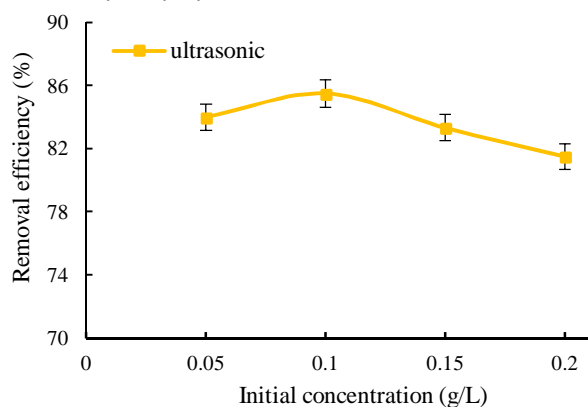


Figure 9. Influence of initial concentration of Ni(II) on its removal efficiency using ultrasonic at $T=25$ °C, $m=6$ g and $pH=9$.

Adsorption isotherms

The adsorption of Ni(II) significantly is affected by the initial concentration of Ni(II) ions in the aqueous solution. In this section, the initial concentration of Ni(II) varies from 0.05 to 0.2 g/L, while the adsorbent dose is 6 g, $pH=9$, and the contact time is 60 min for use of the sono-container. In this section, $m=6$ is selected as the adsorbent dose because according to Figure 8, the efficient dose of adsorbent is 6 g and no significant increase is observed with increasing adsorbent dose of more than 6 g for Ni(II) removal.

Experimental data are adapted to Langmuir and Freundlich isotherm models. Langmuir isotherm model is used to describe the chemical composition and coating of an adsorber layer on the nanoparticles, and its linear form can be expressed by the following equation²⁵⁻²⁷:

$$\frac{C_e}{q_e} = \frac{1}{K_L q_m} + \frac{1}{q_m} C_e \quad (7)$$

Where, q_e is the amount of Ni(II) adsorbed in equilibrium state in mg/g, C_e is equal to the liquid equilibrium concentration of Ni(II) in mg/L, q_{max} and K_L are the Langmuir constants, indicating the adsorbent saturation capacity and K_L is the equilibrium constant related to the affinity of binding sites. q_e is calculated according to equation (2) by measurement C_0 and C_e that are the initial and final equilibrium concentration of Ni(II) ions in solution. By data fitting with the Langmuir model, as shown in Figure 7, $\frac{1}{q_m}$ is equal to 0.5436 that means $q_m = 1.84 \frac{g}{L}$ and $K_L = 3.23 \frac{L}{g}$. The related isotherm parameters evaluated from the nonlinear analyses of the data are given in Table 1.

The Freundlich isotherm model illustrates the distribution of active and energy sites and heterogeneous adsorbent surfaces by the following equation²⁵⁻²⁷:

$$q_e = K_f C_e^{\frac{1}{n}} \quad (8)$$

where, K_f and $\frac{1}{n}$ are Freundlich constants related to absorption capacity and absorption intensity. As shown in Figure 11, in the Freundlich model, the value of K_f is equal to $1.03 \text{ mol}^{1-\frac{1}{n}}\text{L}^{\frac{1}{n}}/\text{g}$. According to Table 1 and Figures 10 and 11, the comparison between these two models shows that both models are well fitted with experimental data, and of course, the value of R^2 is higher in the Langmuir model, and therefore the data compatibility with this model is greater.

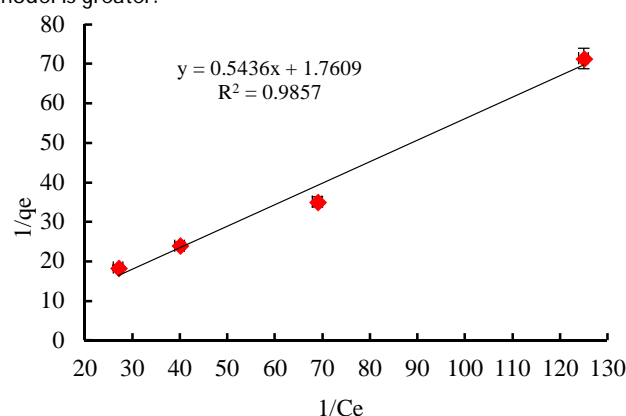


Figure 10. Data fitting by Langmuir adsorption model using ultrasonic at $T=25$ °C, $m=6$ g and $pH=9$.

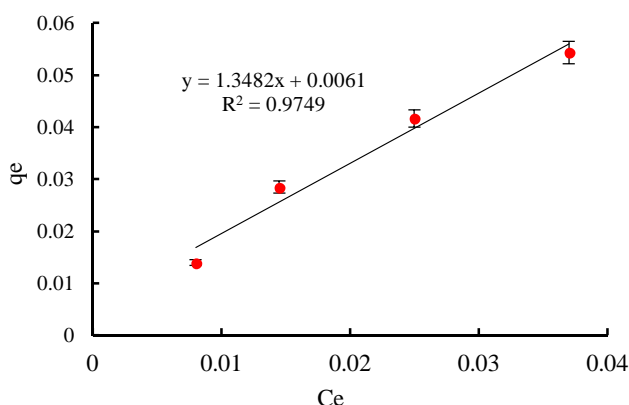


Figure 11. Data fitting by Freundlich adsorption model using ultrasonic at $T=25$ °C, $m=6$ g and $pH=9$.

Conclusions

Experimental investigation of intensifying Ni(II) removal from

aqueous solution by adsorption onto magnetic nanoparticles under the effect of high frequency ultrasonic has been performed. Fe₃O₄ magnetic nanoparticles (MNPs) are synthesized by co-precipitation method and the average size of the nanoparticles is obtained about 19 nm by SEM. A cubic container equipped with five 1.7 MHz ultrasonic transducers has been fabricated to introduce ultrasonic waves into the aqueous solution. The results of Ni(II) removal efficiency and mass transfer characteristics of using ultrasonic are compared with those of shaking. The effects of four independent parameters such as pH, adsorbent mass, initial concentration of Ni(II) and sonication time on the removal efficiency of Ni(II) are investigated. The corresponding results depicted that the optimal pH value is *ca.* 9, which indicates that at this pH, the magnetic adsorbent and nickel metal ions are fully active in the environment. Increasing the adsorbent dose (*m*) cause to increase the adsorption rate of Ni(II) due to the presence of a higher specific surface area of magnetic nanoparticles. In the identical conditions, sonication time for Ni(II) adsorption is lower than the contact time by shaking to reach equal removal efficiency. Indeed, the highest removal efficiency of Ni(II) for the shaker and the sono-container are 83.5% and 85.5%, respectively, with the contact times of 100 minutes and 60 minutes, respectively. It concluded that acoustic and micro-streams generated by high frequency ultrasonic have the high ability to induce mixing and strong mechanical effect inside the sono-container. In addition, microjets induced by high frequency ultrasonic collided with the surface of nanoparticles and so the adsorption of Ni(II) on the adsorbent is increased. The comparison of Langmuir and Freundlich isotherms show that both investigated models are well suited to experimental data and the data compatibility with the Langmuir model is better. From this study, it is found that it is possible to reach the high removal efficiency of Ni(II) by magnetic nanoparticles and high frequency ultrasonic in the little time compared to shaking.

Acknowledgment

The authors would like to thank Islamic Azad University, Kermanshah Branch for providing the support to carry out this work.

References

1. B. Liao, W. Y. Sun, N. Guo, S. L. Ding, S. J. Su, *Colloids Surf. A Physicochem. Eng. Asp.*, 501, **2016**, 32.
2. J. Wang, L. Xu, C. Cheng, Y. Meng, A. Li, *Chem. Eng. J.*, 193, **2012**, 31.
3. F. Fu, Q. Wang, *J. Environ. Manage.*, 92, **2011**, 407.
4. S. Malamis, E. Katsou, *J. Hazard Mater.*, 252, **2013**, 428.
5. S. Sirianuntapiboon, O. Ungkapatatcha, *Bioresour. Technol.*, 98, **2007**, 2749.
6. D. A. Belova, L.Z. Lakshtanov, J.F. Carneiro, S.L.S. Stipp, *J. Contam. Hydrol.*, 170, **2014**, 1.
7. H. Es-sahbany, M. Berradi, S. Nkhili, R. Hsissou, M. Allaoui, M. Loutfi, D. Bassir, M. Belfaquir, M.S. El Youbi, *Mater Today Proc.*, 13, **2019**, 866.
8. Y. Song, G. Wang, B. Yang, Y. Wang, *Hydrometallurgy*, 180, **2018**, 246.
9. E. S. Menkah, N. Y. Dzade, R. Tia, E. Adei, N. H. de Leeuw, *Appl. Surf. Sci.*, 480, **2019**, 1014.
10. M. Jamshidi, M. Ghaedi, K. Dashtian, A.M. Ghaedi, S. Hajati, A. Goudarzi, *Spectrochim. Acta A Mol. Biomol. Spectrosc.*, 153, **2016**, 257.
11. J. Ji, X. Lu, Z. Xu, *Ultrasonic. Sonochem.* 13, **2006**, 463.
12. J. P. d. S. Fernandes, B. S. Carvalho, C. V. Luhez, M. J. Politi, C. A. Brandt, *Ultrasonic. Sonochem.*, 18, **2011**, 489.
13. O. Hamdaoui, E. Naffrechoux, *Ultrasonic. Sonochem.*, 16, **2009**, 15.
14. A. Asfaram, M. Ghaedi, S. Hajati, A. Goudarzi, A. A. Bazrafshan, *Spectrochim. Acta A Mol. Biomol. Spectrosc.*, 145, **2015**, 203.
15. F. Parvizian, M. Rahimi, N. Azimi, *Chem. Eng. Process.*, 57, **2012**, 8.
16. M. Rahimi, N. Azimi, F. Parvizian, *Chem. Eng. Process.* 70, **2013**, 250.
17. R. Mondragon, J. E. Julia, A. Barba, J. C. Jarque, *Powder Technol.*, 224, **2012**, 138.
18. X. L. Zou, T. Zhou, J. Mao, X. H. Wu, *Chem. Eng. J.*, 257, **2014**, 36.
19. B. S. Schueller, R. T. Yang, *Ind. Eng. Chem. Res.*, 40, **2001**, 4912.
20. Y. Wu, Y. Han, Y. T. Fan, D. T. Chu, X. Ye, M. Ye, G. Xie, *Ultrasonic. Sonochem.*, 48, **2018**, 311.
21. F. Mehrabi, E. A. Dil, *Ultrasonic. Sonochem.*, 37, **2017**, 37.
22. H. A. Eivari, A. Rahdar, H. Arabi, *Int. J. Sci. Eng. Invest.*, 1, **2012**, 70.
23. Y. Xing, Y. Y. Jin, J. C. Si, M. L. Peng, X. Wang, C. Chen, Y.L. Cui, *J. Magn. Mater.*, 380, **2016**, 150.
24. A. M. Khan, F. Shafiq, S. A. Khan, S. Ali, B. Ismail, A. S. Hakeem, A. Rahdar, M. F. Nazar, M. Sayed, A. R. Khan, *J. Mol. Liq.*, 274, **2019**, 673.
25. W. Yan, T. Xiao-wu, W. Heng-yu, *J. Cent. South Univ.*, 22, **2015**, 4184.
26. Z. Mokadem, S. Mekki, S. Saïdi-Besbes, G. Agusti, A. Elaissari, A. Derdour, *Arab. J. Chem.*, 10, **2017**, 1039.
27. T. Shojaeimehr, F. Rahimpour, M. A. Khadivi, M. Sadeghi, *J. Ind. Eng. Chem.*, 20, **2014**, 870.